ELSEVIER

International Journal of Mass Spectrometry 219 (2002) 253–267

International Journal of Mass Spectrometry

www.elsevier.com/locate/ijms

Analysis of protein mixtures by matrix-assisted laser desorption ionization-ion mobility-orthogonal-time-of-flight mass spectrometry

Brandon T. Ruotolo[a], Kent J. Gillig[a], Earle G. Stone[a], David H. Russell[a,*], Katrin Fuhrer[b], Marc Gonin[b], J. Albert Schultz[b]

[a] *Laboratory for Biological Mass Spectrometry, Department of Chemistry, Texas A&M University, College Station, TX 77843, USA*
[b] *Ionwerks, Inc., 2472 Bolsover, Suite 255, Houston, TX 77005, USA*

Received 3 July 2001; accepted 6 November 2001

Abstract

Matrix-assisted laser desorption ionization (MALDI)-ion mobility (IM)-time-of-flight (TOF) mass spectrometry (MS) has been applied to the analysis of enzymatically digested protein mixtures. The IM-TOF MS technique is rapid relative to other approaches to coupling separation methods with mass spectrometry (e.g., LC–MS, CE–MS, etc.), and MALDI-IM-TOF MS retains the advantage of reduced chemical noise which makes chromatography–mass spectrometry such a powerful analytical method. The use of IM separation prior to mass analysis also facilitates the use of internal calibration. MALDI-IM-TOF MS was evaluated by analyzing low picomole amounts of single proteins and mixtures of proteins digested with trypsin, without using time consuming "clean-up" procedures (e.g., lyophilization, dialysis, etc.). In all cases, a larger number of predicted digest fragments and higher amino acid coverages are obtained by MALDI-IM-TOF MS when compared with a conventional MALDI-TOF MS analysis. There also appears to be less signal suppression in high pressure MALDI compared to high vacuum MALDI. For example, the ratio of lysine-to-arginine terminated digest fragments appears to be higher in high-pressure MALDI relative to high-vacuum MALDI. (Int J Mass Spectrom 219 (2002) 253–267)

Keywords: Peptide mass mapping; Protein digest; Enzymatic digestion; Mass-mobility correlations; MALDI ion suppression

1. Introduction

The growing interest in proteomics underscores the need for analytical techniques with increased efficiency and sensitivity [1–5]. Current methodologies for analyzing protein mixtures (rather than a single protein) are based on protocols originally introduced by Henzel et al. [6] in which the protein constituents of a sample are separated by 2D gel electrophoresis, each individual spot on the gel is digested, and the peptide mass map is acquired by MALDI mass spectrometry [7,8]. Although this method has been proven to be analytically useful, the process is time consuming, labor intensive, and relatively irreproducible. Improving upon this experiment has been a focus of many research groups over the past decade. For example, our laboratory has presented a decompartmentalized methodology involving micro-tip separation and enzymatic digestion. When combined with thermal denaturation, this methodology reduces analysis

* Corresponding author. E-mail: russell@mail.chem.tamu.edu

1387-3806/02/$ – see front matter
PII S1387-3806(01)00583-8

time and provides increased sensitivity [9,10]. We have also shown that proteolysis in organic solvents can accelerate protein digestion, and further streamline the analysis of protein digests [11]. In addition to these techniques, significant advances have been made in interfacing HPLC and CE to mass spectrometry (via electrospray ionization) [12–16]. However, these techniques suffer from insufficient detection limits for most proteomic applications, and a low tolerance toward buffers and salts [17].

Recently, we reported on the utility of MALDI-ion mobility for the separation of peptide mixtures prior to TOF mass analysis [18,19], and we have shown that IM-TOF coupled with surface-induced dissociation (SID) can be used to simultaneously acquire a peptide mass map and peptide sequence information [20]. An advantage of IM-TOF MS is the compatibility of the separation and mass analysis methods. For example, ion mobility separations carried out at relatively low pressure (ca. 10 Torr) facilitate interfacing IM to the high vacuum region of the mass spectrometer, and rapid separation (10–1 ms) is compatible with the data acquisition rates of TOF mass analyzers [19].

In the low field limit, ion mobility separation is based on the relationship between the ion's drift velocity (v_d) and the electric field strength (E):

$$K = \frac{v_d}{E} \tag{1}$$

where K is the mobility of an ion in a neutral bath gas. Drift time through the mobility cell (K^{-1}) varies with reduced mass (m), collision cross-section (W), and charge state (z) of the ion as illustrated in Eq. (2)

$$K^{-1} \alpha (\mu^{1/2}) \left(\frac{\Omega}{z} \right). \tag{2}$$

For a series of large, structurally related ions having the same charge, e.g., singly charged peptide ions with m/z values of ca. 500–2000, μ is virtually constant and K^{-1} is controlled by Ω. Although Ω contains terms for both hard-sphere collision and ion–neutral interaction potential, the interaction potential term is negligible for large ions [19], and mobility is a function of the ion's collision cross-section-to-charge (Ω/z) ratio. A plot of K^{-1} vs. m/z is near linear and can be used to predict elution order and identify ions or groups of ions [20,21]. We see the predictable, near-linear relationship of K^{-1} and m/z as an analytical advantage over techniques such as high-field asymmetric waveform ion mobility spectrometry [22], where no such predictable value can be associated with the elution time. Techniques that separate analytes based on a property that has a direct relationship with mass, such as GC and PAGE, are routinely used to increase the predictability of MS results [6,23].

Recent experiments further illustrate the utility of ion mobility-mass spectrometry for protein and protein mixture analysis. For example, using ion mobility separation we detect a much higher percentage of digest fragments resulting in an increase in the observed amino acids present in a protein sequence (percent coverage). Our current work focuses on the benefits this increased sensitivity can provide for the analysis of complex mixtures of digested protein. This paper compares results obtained by MALDI-ion mobility-mass spectrometry and conventional MALDI-TOF currently used in our laboratory [24]. Although IM can be used to determine the conformation of ions in the gas-phase [25,26], the focus of this work is the increased sensitivity of MALDI-IM-TOF MS for mass mapping. Ion mobility separation prior to mass analysis significantly increases the dynamic range for ion detection and allows the use of internal calibrants for complex mixture analysis.

2. Experimental

All proteins (horse heart cytochrome *c*, chicken egg white lysozyme, bovine serum albumin, bovine hemoglobin α, and bovine hemoglobin β) were purchased from Sigma and sequence grade modified trypsin was purchased from Promega (Madison, WI).

The protein digest methods used for these studies have been previously described [9,23]. Briefly, protein samples were dissolved in 50 mM ammonium bicarbonate (Sigma) and the protein mixtures were thermally denatured at 90 °C for 20 min. Following this step, samples were placed in an ice

bath in order to quench the denaturation process. The single-component protein samples were digested without using thermal denaturation. All samples were digested with sequencing grade modified trypsin at 37 °C for 4–5 h. The concentration of trypsin was maintained at 40:1 (weight of substrate/weight of trypsin) for all experiments.

The high resolution MALDI-TOF analysis was performed using a PerSeptive Biosystems Voyager Elite XL TOF equipped with a pulsed nitrogen laser (337 nm) in the reflected, delayed extraction (DE) mode as described previously [24]. In addition, all samples analyzed using this technique were prepared using the α-cyano-4-hydroxycinnamic acid overlayer method [24]. This procedure was selected because it maximized resolution, reproducibility, amino acid coverage, and sensitivity for protein digest samples.

The MALDI-ion mobility-o-time-of-flight-mass spectrometer (Fig. 1) is composed of a 4 cm drift tube that is maintained at a pressure of 1–10 Torr helium, resulting in an E/N value of ca. 10 V cm^{-1} Torr^{-1} (where E is the applied electric field and N is the gas number density in the drift tube). Under these conditions, the mobility resolution is ca. 25. Resolution is expressed in terms of drift time over peak width (full width at half maximum height). The ions exit the mobility drift tube and enter the ion source of a 20 cm TOF mass spectrometer capable of ca. 400 mass resolution. TOF spectra were acquired at IM drift time intervals of 2 μs to insure complete sampling of the eluting mobility profiles.

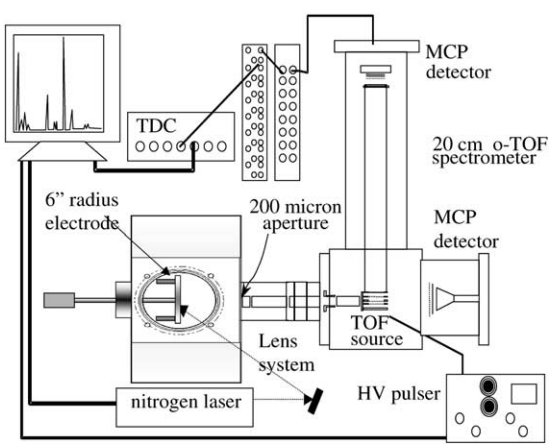

Fig. 1. Schematic diagram of the MALDI-IM-o-TOF MS apparatus.

Sample preparation for IM-TOF MS involves taking 1 μL containing 1–10 picomoles of the digested protein and diluting it with a solution of 2′,4′,6′-trihydroxyacetophenone (Sigma) in HPLC grade methanol (Fischer) to reach a matrix to analyte ratio of roughly 1000:1. In addition, fructose is added to this mixture (in a 1:1 ratio with the matrix) to increase the number of single-shot spectra that can be taken before the sample spot is depleted, i.e., the durability of the sample is increased [27–29]. The analyte was then spotted onto a stainless steel probe tip in a dried droplet fashion and inserted into the back electrode of the ion mobility cell. No additional clean-up steps were used to prepare the sample. Sample preparation procedures were optimized in terms of resolution, sensitivity, reproducibility, and amino acid coverage for MALDI of digested protein performed at 10 Torr He.

Calibration of the mass spectrometer was performed both internally and externally during the course of these experiments. For internal calibration, the isotope averaged masses of C_{60}^+ (720.642 amu) and C_{70}^+ (840.749 amu) ions were used. The mass–mobility relationship for peptide ions is very different from the mass–mobility relationship for C_{60} and C_{70} (Aldrich) as shown in Fig. 2. Thus, the signals for analyte and calibrant are easily differentiated. For these experiments, C_{60}/C_{70} was co-deposited in trace amounts with peptide mixtures in order to avoid the suppression of peptide ionization.

Data analysis was performed using Grams/32 software utilizing both three-dimensional and contour style plots displaying m/z vs. mobility drift time (uncorrected for transit time through the lens system of the instrument). Data was accumulated for a period of 1 min (operating the laser at 20 Hz) to assure a representative spectrum. Peaks in the protein digest spectra were manually assigned on the basis of signal-to-noise (S/N) ratios (minimum 5/1) and mass accuracy (+/− 1 mass unit). Spectra were analyzed primarily for the presence of $[M + H]^+$ ions, and salt adducts

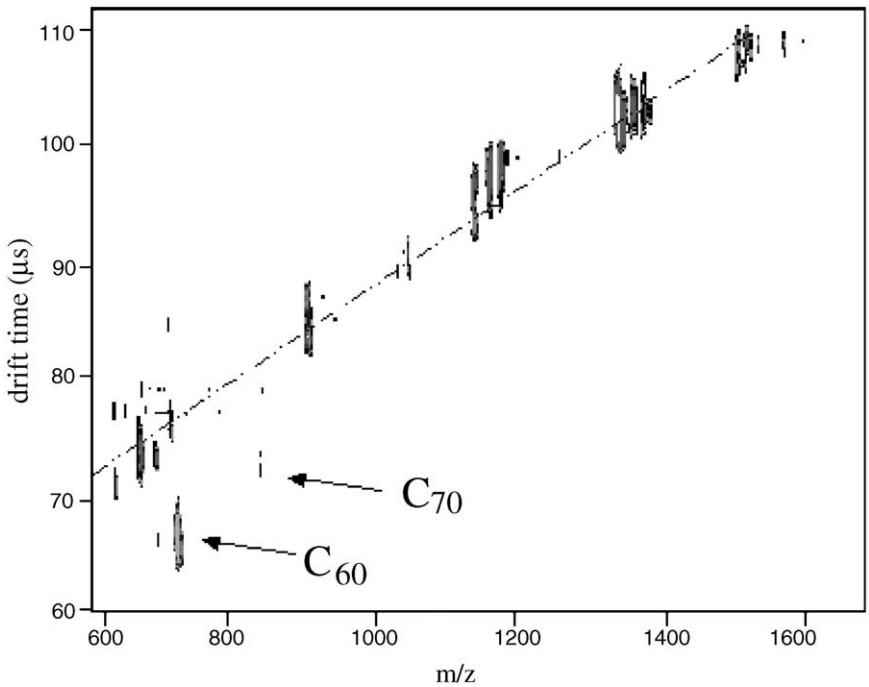

Fig. 2. Contour plot of drift time vs. *m/z* for six peptides: HLGLAR ($m/z = 666.8$), des-arg^9-bradykinin ($m/z = 905.0$), and gramicidin s ($m/z = 1143.4$), substance p ($m/z = 1347.6$), RRLIEDAEYAARG ($m/z = 1519.7$) utilizing C_{60} ($m/z = 720.642$) and C_{70} ($m/z = 840.749$) for internal calibration. The dotted line (denoting the linear approximation of the peptide mass–mobility relationship in this mass range) is added to guide the eye.

($[M + Na]^+$ and $[M + K]^+$) were used as a means of further confirmation. Under the separation conditions used in these experiments, alkali adducted peptide ions co-elute with their respective $[M+H]^+$ ions. Theoretical digest fragment masses were obtained using the University of California, San Francisco MS-Digest Program (utilizing the SwissProt Database) specifying one missed cleavage in the case of bovine serum albumin, two missed cleavages in the cases of horse heart cytochrome *c* and chicken egg white lysozyme, and three missed cleavages in the cases of bovine hemoglobin α and bovine hemoglobin β [30].

3. Results

Tryptic digests of several single-component protein samples (horse heart cytochrome *c*, chicken egg white lysozyme, and bovine serum albumin) were analyzed. The 3D plot of *m/z* vs. ion mobility drift time (in ms) for horse heart cytochrome *c* is shown in Fig. 3. This plot contains 16 identifiable peptide fragments (13 lysine and 3 arginine terminated digest fragments), which corresponds to 70% amino acid coverage. The sequence coverage obtained from an analysis of the data shown is listed in Table 1. Similar data for bovine serum albumin is presented in Fig. 4. From this data, we were able to identify 45 digest fragments (32 lysine and 13 arginine terminated digest fragments), which corresponds to an amino acid coverage of 66%. The complete analysis of the data, including sequence coverage, is itemized in Table 2.

A 1:1 mixture of bovine hemoglobin α and bovine hemoglobin β was digested with trypsin and analyzed by IM-TOF-MS (Fig. 5). We can identify 22 digest fragments that are assigned to the hemoglobin

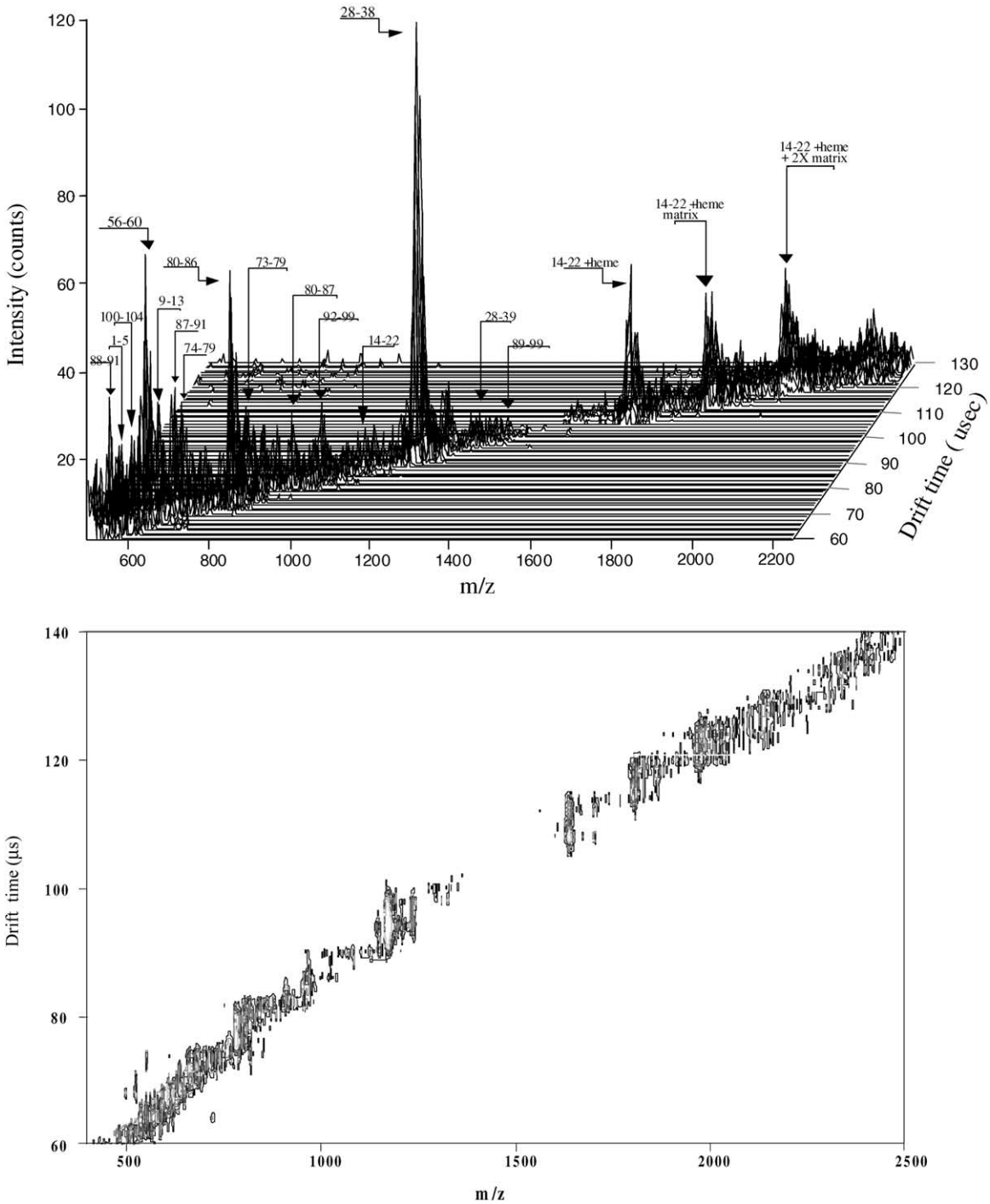

Fig. 3. 3D plot of *m*/*z* vs. IM drift time of a tryptic digest of thermally denatured horse heart cytochrome *c* (top). A contour plot representation of the same dataset (bottom).

Table 1
List of the observed fragments from a tryptic digest of cytochrome *c* (spectrum shown in Fig. 3)

Position	Experimental mass	Theoretical mass	Position	Experimental mass	Theoretical mass
88–91	534.4	533.6	73–79	807.7	807.0
1–5	548.4	547.6	80–87	908.5	908.2
100–104	563.5	562.6	92–99	966.1	965.1
56–60	605.1	604.7	14–22	1018.9	1019.2
9–13	634.0	634.8	28–38	1170.2	1169.3
87–91	661.2	661.8	28–39	1296.7	1297.5
74–79	678.3	678.8	89–99	1352.5	1351.5
80–86	780.6	780.0	14–22 + heme	1634.6	1634.9

Table 2
List of the observed tryptic digest fragments of bovine serum albumin (spectrum shown in Fig. 4)

Position	Experimental mass	Theoretical mass	Position	Experimental mass	Theoretical mass	Position	Experimental mass	Theoretical mass
25–28	501.0	500.5	548–557	1144.4	1143.4	437–451	1641.8	1640.9
558–561	510.3	509.6	236–245	1147.3	1146.3	249–263	1694.7	1694.0
101–105	546.0	545.7	66–75	1164.3	1164.3	387–401	1740.4	1739.9
219–222	572.9	572.7	246–256	1296.0	1295.5	508–523	1824.9	1825.1
223–228	649.4	649.8	402–412	1306.8	1306.5	123–138	1846.0	1846.0
156–160	665.9	665.8	558–568	1309.4	1309.5	281–297	1887.1	1886.1
236–241	689.9	689.8	360–371	1441.6	1440.7	89–105	1891.1	1890.2
29–34	713.1	712.8	421–433	1479.7	1480.7	101–117	1892.6	1892.1
341–346	753.3	752.8	483–495	1483.7	1483.8	438–455	1897.6	1898.2
562–568	818.2	818.9	387–399	1497.6	1498.6	139–155	1964.5	1964.2
483–489	842.7	842.0	549–561	1504.8	1505.8	168–183	2047.3	2046.3
161–167	928.3	928.1	139–151	1520.8	1520.7	341–359	2303.3	2302.5
310–318	1017.1	1016.2	347–359	1568.6	1568.7	131–151	2387.9	2388.7
588–597	1050.5	1051.2	361–374	1596.8	1596.9	508–528	2415.0	2415.7
223–232	1140.3	1139.3	184–197	1634.4	1634.8	469–489	2493.0	2492.0

Table 3
List of the observed fragments from a tryptic digest of a mixture of hemoglobin α and hemoglobin β (spectrum shown in Fig. 5)

Hemoglobin α			Hemoglobin β		
Position	Experimental mass	Theoretical mass	Position	Experimental mass	Theoretical mass
12–16	533.2	532.6	61–65	541.4	540.6
62–68	672.9	673.8	8–18	1177.4	1178.4
91–99	1087.4	1088.3	65–75	1225.9	1226.4
57–68	1123.6	1124.3	116–131	1869.8	1870.1
128–139	1280.0	1280.5	65–81	1949.3	1948.2
17–31	1529.6	1530.6	76–94	2115.1	2114.4
41–61	2285.2	2285.5	8–29	2262.4	2261.6
8–31	2443.4	2442.7	40–60	2318.2	2318.6
17–40	2583.1	2583.9	19–39	2358.1	2358.7
69–92	2636.8	2638.0	40–65	2712.8	2712.1
100–127	2970.5	2971.4	95–119	2793.2	2793.3

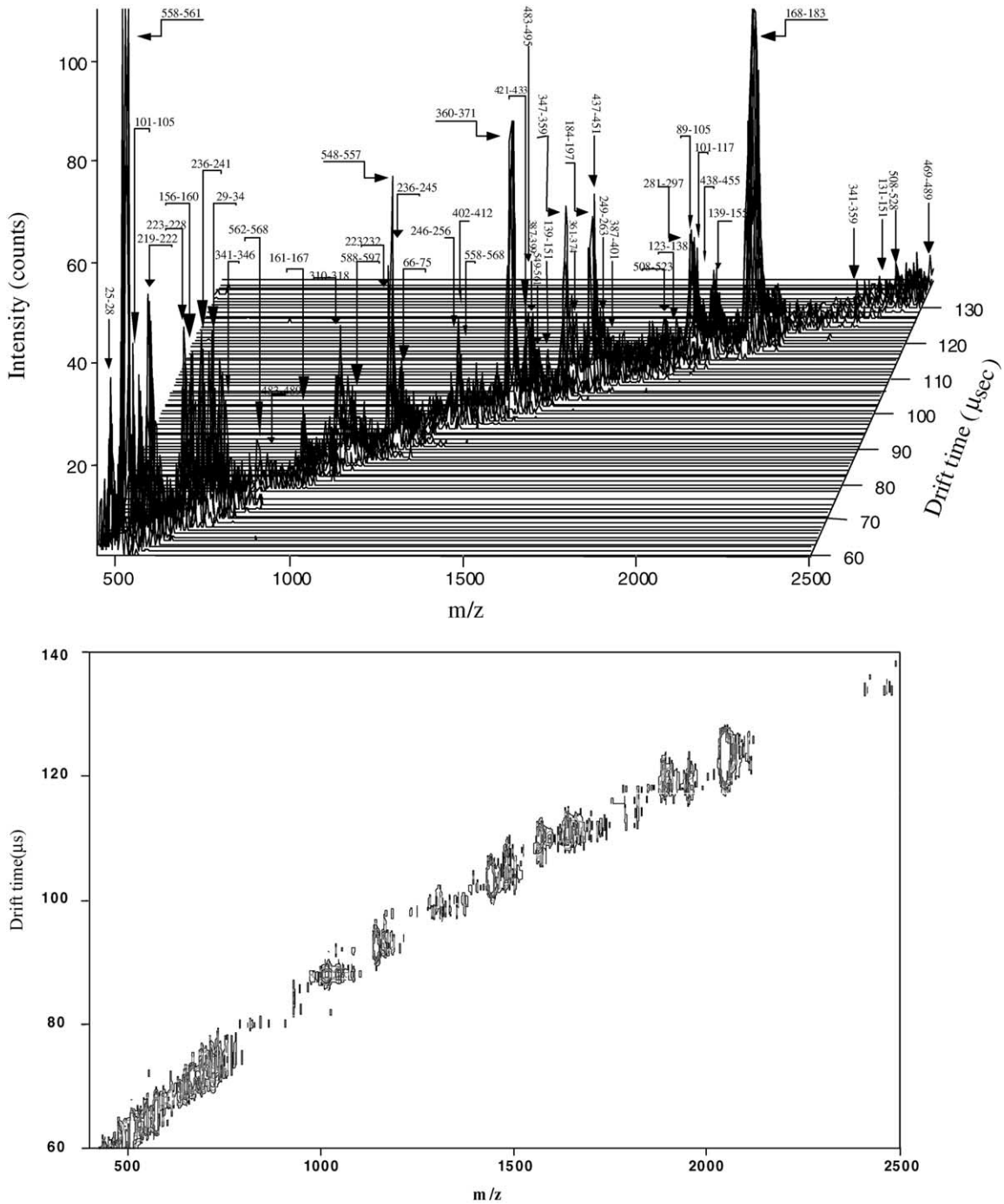

Fig. 4. 3D plot of *m*/*z* vs. IM drift time of a tryptic digest of thermally denatured bovine serum albumin (top). A contour plot representation of the same dataset (bottom).

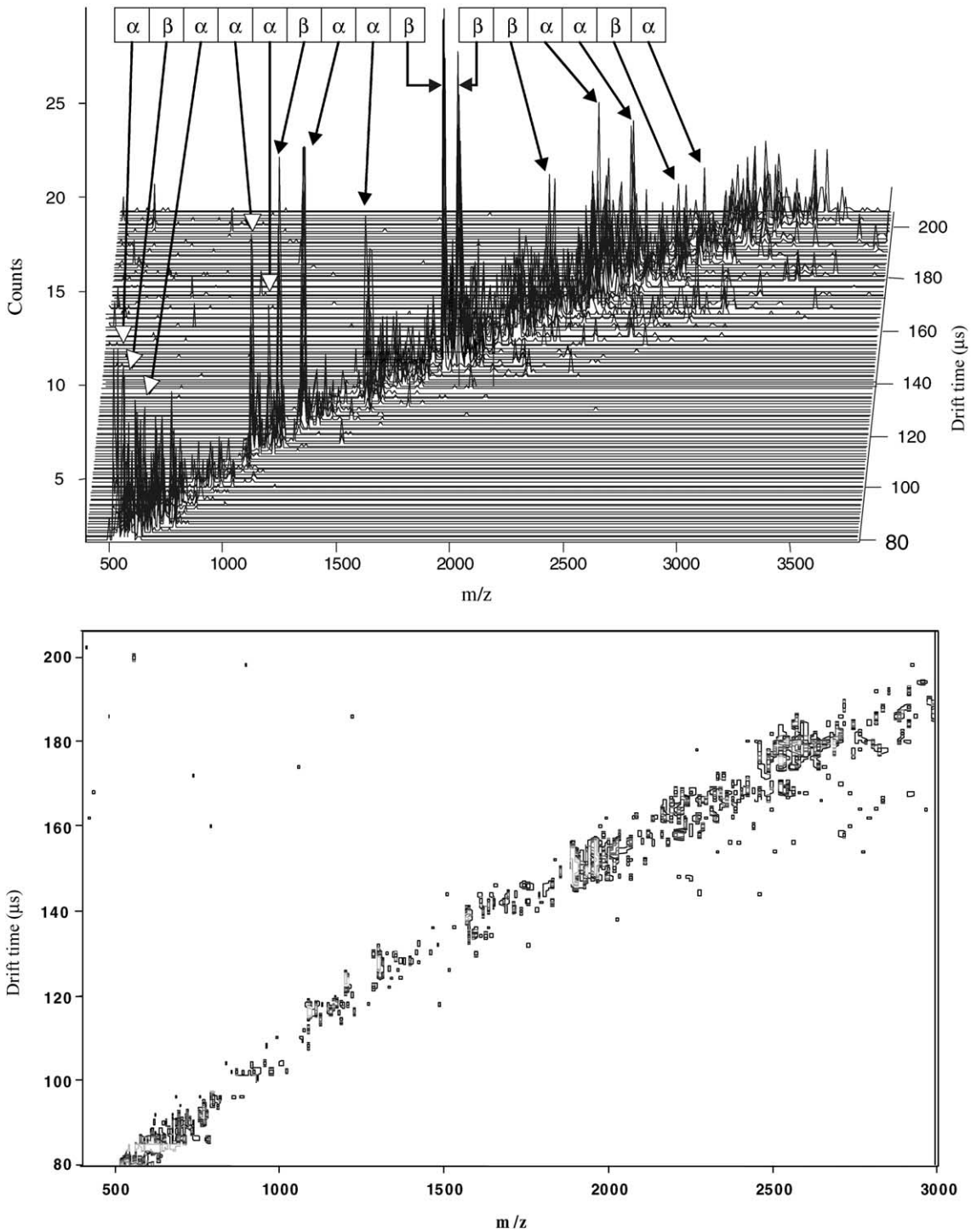

Fig. 5. 3D plot of *m*/*z* vs. IM drift time of a tryptic digest of a thermally denatured mixture of bovine hemoglobin α and bovine hemoglobin β (top). A contour plot representation of the same dataset (bottom).

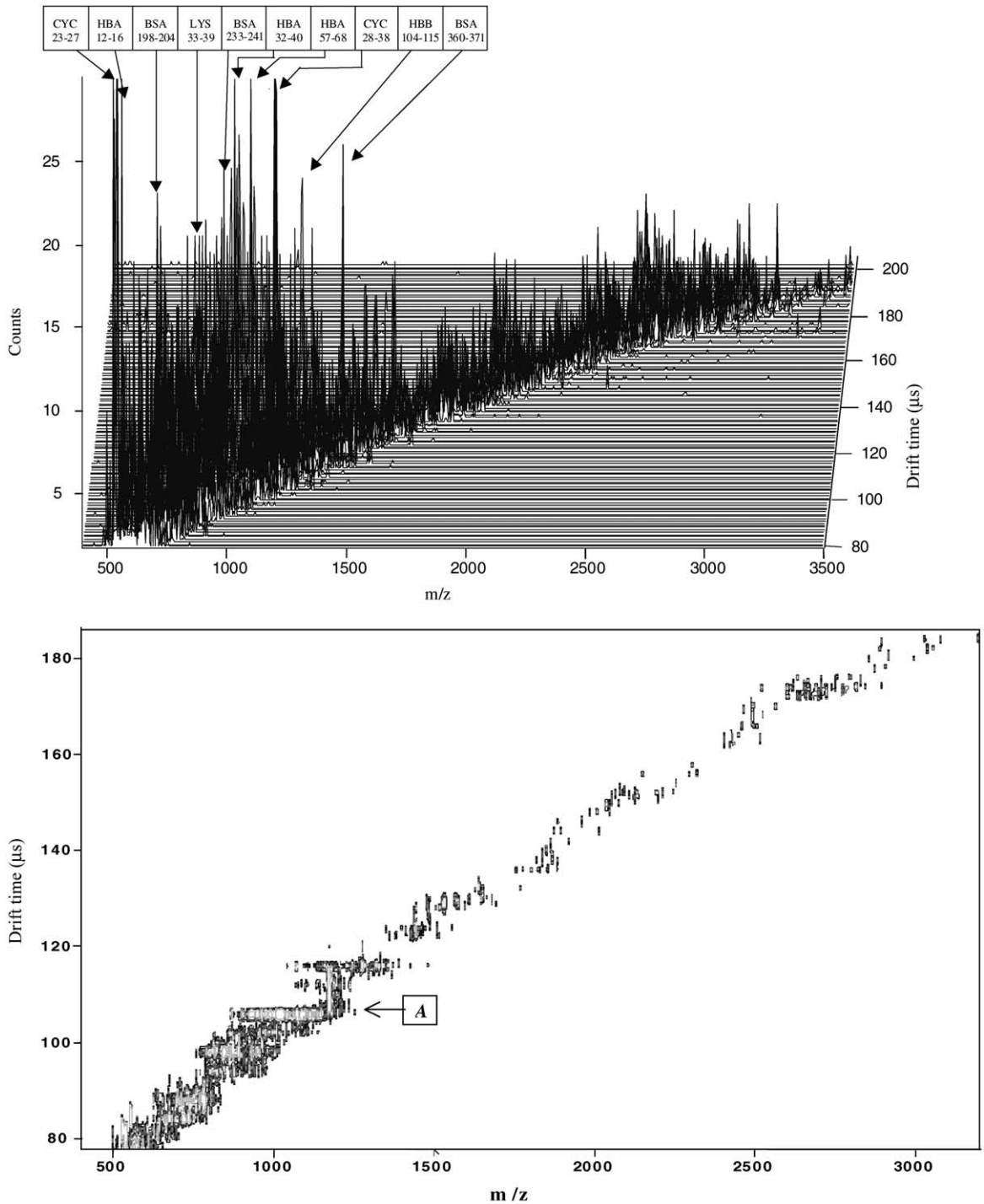

Fig. 6. 3D plot of *m*/*z* vs. IM drift time of a tryptic digest of a thermally denatured mixture of horse heart cytochrome *c*, chicken egg white lysozyme, bovine serum albumin, bovine hemoglobin α, and bovine hemoglobin β (top). A contour plot representation of the same dataset (bottom). Point A is an area of unresolved digest fragments (discussed in text).

Table 4
List of selected fragments observed from a tryptic digest of a five-component protein mixture (spectrum shown in Fig. 6)

Serum albumin			Lysozyme			Cytochrome *c*			Hemoglobin α			Hemoglobin β		
Position	Experimental mass	Theoretical mass	Position	Experimental mass	Theoretical mass	Position	Experimental mass	Theoretical mass	Position	Experimental mass	Theoretical mass	Position	Experimental mass	Theoretical mass
229–232	508.5	508.5	19–23	607.2	606.7	23–27	527.2	526.6	61–65	541.1	540.6	12–16	532.7	532.6
29–34	713.0	712.8	33–39	874.6	874.9	1–7	733.0	732.8	1–7	822.5	821.9	8–16	931.4	931.1
221–228	920.1	919.1	135–143	1046.8	1046.2	28–38	1168.5	1169.3	19–29	1102.6	1102.2	57–68	1123.5	1124.3
139–151	1519.8	1520.7	116–130	1677.8	1676.9	61–72	1495.8	1496.7	30–39	1275.6	1275.5	128–139	1281.5	1280.5
469–489	2491.6	2492.0	92–115	2465.9	2466.9	56–73	2210.5	2210.5	66–94	3193.3	3193.6	12–31	2044.0	2044.2

subunits: 11 from hemoglobin α (3 arginine and 8 lysine terminated) and 11 from hemoglobin β (2 arginine and 9 lysine terminated). The identified fragments correspond to an amino acid coverage of 94% for both proteins. A complete list of the identified digest fragments is given in Table 3.

The tryptic digest of a five-component protein mixture consisting of horse heart cytochrome *c*, chicken egg white lysozyme, bovine serum albumin, bovine hemoglobin α, and bovine hemoglobin β was also analyzed. The resultant three-dimensional spectrum is shown in Fig. 6, and Table 4 contains the sequence coverage for this dataset. Amino acid coverages for the protein digest components were: 100% for horse heart cytochrome *c*, 89% for chicken egg white lysozyme, 69% for bovine serum albumin, 52% for bovine hemoglobin α, and 87% for bovine hemoglobin β. An overall sequence coverage of 75% (853 amino acids observed out of 1144 total) was obtained for the protein mixture.

4. Discussion

A major advantage of TOF-MS is that mass analysis can be carried out very rapidly which facilitates high-throughput applications. On the other hand, accurate mass measurement requires the use of internal calibrants, which can be problematic for protein digests due to the large number of ion signals (spectral congestion) and ion suppression effects [24,31]. Consequently, external calibration is typically used for peptide mass mapping, limiting both mass accuracy and sample throughput. The data presented in Fig. 2 illustrates a unique feature of IM-MS that could substantially increase the utility of peptide mass mapping. Note that the mass–mobility relationship for C_{60} and C_{70} is very different than it is for peptide ions. For a series of structurally related compounds, a plot of K^{-1} vs. m/z is near linear (mass–mobility plot). Thus, it is possible to choose a calibrant that is structurally different from the series of analyte ions, and employ the mobility differences to distinguish calibrant and analyte signals. This procedure can be used to eliminate mass overlap and ion suppression effects that currently limit the application of internal calibration for complex mixture analysis.

The utility of separation-mass spectrometry techniques for reduction of background signals (chemical noise) provides many applications for GC–MS and tandem MS [32]. Ion mobility separation can be used to achieve similar results. For a homologous series of singly charged ions, the near-linear relationship between drift time and m/z can be used to eliminate signals that lie off the analyte trend-line. For example, tryptic digest fragments fall along a recognizable trend-line, allowing these signals to be easily discerned from chemical noise that appears off of the peptide trend-line.

Mass–mobility trend-lines greatly assists in the identification of ion signals, i.e., peak picking, in peptide mass mapping experiments. Typically, the confidence level for assigning weak signals is low, because there is only a single dimension of information (m/z) available. In a high-resolution peptide mass-mapping experiment, the isotope cluster can facilitate peak picking; however, this is not always free of ambiguity [33]. The addition of a second dimension (i.e., mass–mobility) allows for the classification of ion signals as peptide ions, thus, greatly increasing the confidence level for such assignments.

The data presented in Figs. 3 and 4 demonstrate the utility of MALDI-IM-TOF MS direct analysis of protein digest samples. Note that most of the peptide ions observed fall along a single mobility trend line, as expected for a series of structurally related ions under conditions where drift time depends primarily on Ω/z ratio. It is also important to note that multiply charged species are not observed by MALDI of tryptic peptides, which eliminates the possibility of multiple analyte trend-lines in the data [34]. Both of the single-component spectra contain a high number of identified digest fragments relative to that typically observed using high-vacuum MALDI-TOF MS [9]. There is generally good correlation between the dominant fragments observed in both MALDI-TOF and MALDI-IM-TOF techniques, however, we identify a greater number of digest fragments using

MALDI-IM-TOF. The reason(s) for increased percent coverage could be due to several factors. Quite possibly, the increased percent coverage is a direct result of the mobility separation. Ion mobility separation facilitates both detection (by reduction of the chemical background) and assignment (as to peptide origin) of ion signals of low abundance [32]. In a typical digest, lower abundance fragment ions can result from missed cleavages in the digestion process, and these fragment ions are oftentimes larger and more sequence informative than are smaller fragments [35]. Another possibility stems from the ionization conditions used in the MALDI-IM-TOF instrument. For instance, MALDI at elevated pressures could provide "softer" ionization conditions as well as collisional stabilization [36]. Alternatively, the single ion counting detection system employed by the MALDI-IM-MS instrument is more sensitive than is the method utilized by more conventional MALDI-TOF MS instruments (i.e., current integration). Overall, the mobility technique consistently detects both a higher number of digest fragment ions overall, and a higher number of larger digest fragment ions (greater than 2000 amu) than does high-vacuum MALDI-TOF.

Many protein samples are mixtures, or contain multimer complexes, e.g., ribosomes, which complicate sample handling/preparation for techniques that are unable to deal with such complex samples. To illustrate the utility of MALDI-IM-TOF MS for such samples, we analyzed both a two- and five-component protein mixture. The data for the two-component mixture, consisting of bovine hemoglobin α and bovine hemoglobin β, contains a high percentage (see Table 3) of the total possible amino acids present in the sample (94% coverage for both protein sub-units). In addition, the resulting amino acid coverages obtained are higher than those observed using high-vacuum MALDI-TOF MS. When compared with an optimized (in terms of sample preparation and MALDI matrix choice) MALDI-TOF analysis of the same mixture [9], we find that the ion mobility technique generates approximately 20% more amino acid coverage than high-vacuum MALDI-TOF MS. It is also important to note that ion suppression of one of the protein sub-units is insignificant in either the MALDI-TOF or MALDI-IM-TOF spectra.

The data obtained from the more complex protein digest sample (Table 4; Figs. 6 and 7) also contain a very high amino acid coverage. However, the drift cell does not provide complete separation for all peptide ions, e.g., see the section labeled A in Fig. 6. Also of note, the percent coverage for horse heart cytochrome *c* increases from 70% (pure protein) to 100% (in mixture). Several factors contribute to this increase. We have observed, on a limited basis, that sample-to-sample variability in MALDI (i.e., variability in the digestion process, the crystallization process, the inclusion of the analyte in the matrix, etc.) can cause differences in both the identity and intensity of the peaks observed. Such variations could influence peak picking and account for the observed increase in percent coverage observed for cytochrome *c*. Typically, when analyzing a sample of this level of complexity by MALDI-TOF MS, the signals for certain digest fragments are suppressed. Krause et al. suggest that ion suppression is most often observed

Table 5
A comparison of MALDI-IM-TOF (on top in italics) and MALDI-TOF (on bottom in bold) data for a mixture of five proteins

	BSA (%)	LYS (%)	CYC (%)	HBB (%)	HBA (%)	Total (%)
Arg terminated	*55*	*43*	*60*	*38*	*20*	*45*
Fragments	**21**	**3.6**	**60**	**0**	**20**	**12**
Lys terminated	*48*	*36*	*52*	*24*	*22*	*40*
Fragments	**5.3**	**0**	**16**	**2.4**	**0**	**5.7**
Amino acid	*69*	*89*	*100*	*87*	*52*	*75*
Coverage	**20**	**4.8**	**61**	**4.1**	**11**	**18**

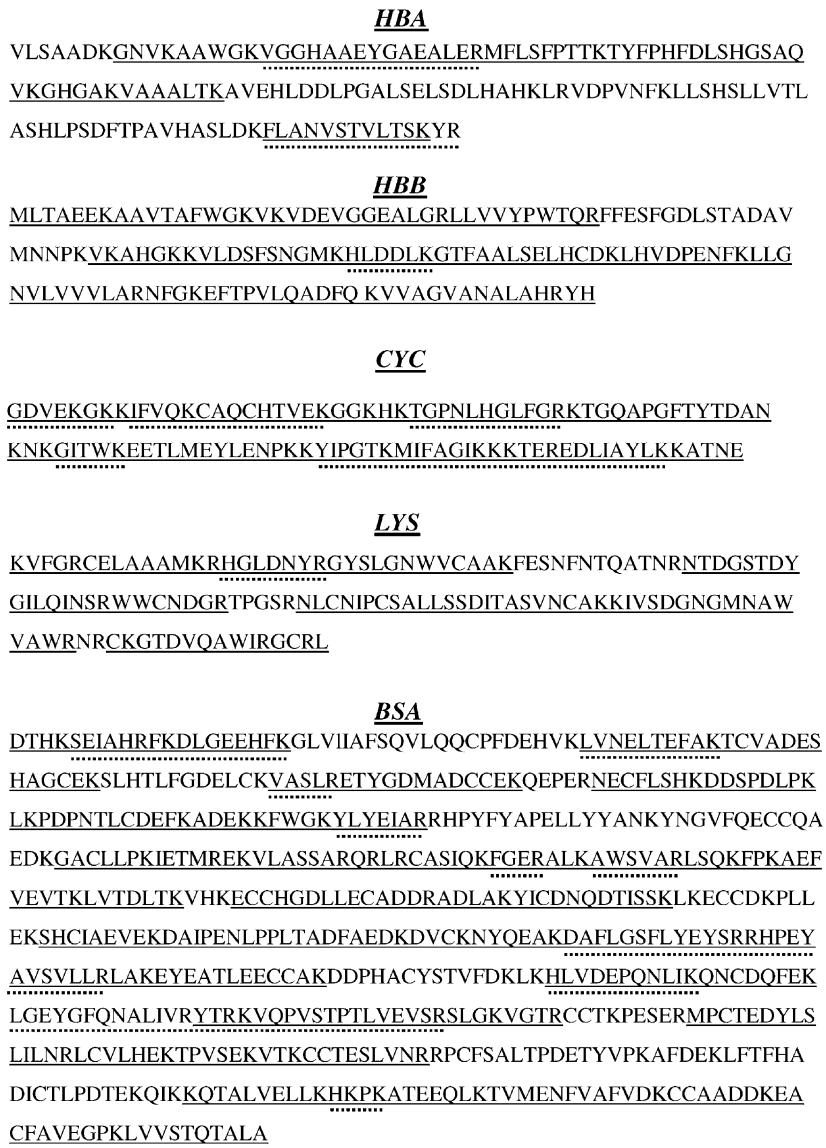

Fig. 7. Sequence coverage information pertaining to the mixture of five proteins referred to in text. Abbreviations: HBA, hemoglobin α, HBB, hemoglobin β, CYC, cytochrome *c*, LYS, lysozyme, BSA, bovine serum albumin. A solid line underlines coverage for the MALDI-IM-TOF experiment, and a dashed line denotes the coverage obtained by high-vacuum MALDI-TOF.

in conjunction with lysine terminated digest fragments [37]. This effect is illustrated by data shown in Table 5, where we compare data obtained using MALDI-TOF and MALDI-IM-TOF analysis of the same five-component protein digest mixture. The MALDI-IM-TOF data yields greater amino acid coverages for all of the protein constituents present in the sample. In this case, the increase in amino acid coverage can be linked to the apparent lack of suppression of lysine terminated digest fragments in the spectrum. This observation is supported by data for cytochrome *c*, where the same percentage of arginine terminated

digest fragments (60%) are detected by MALDI-TOF and MALDI-IM-TOF, but very different percentages of the predicted lysine terminated digest fragments (52% for the ion mobility technique and 16% for the typical MALDI-TOF protocol) are detected. The data for hemoglobin α also illustrates a similar effect. Again, the same percentage of theoretically predicted arginine terminated digest fragments are observed in both methods, but none of the predicted lysine terminated digest fragments are observed in the standard MALDI-TOF protocol, whereas 20% are observed using the ion mobility protocol. The lack of suppression coupled with the reduced chemical noise in the IM-TOF MS spectrum increases the number of detected amino acids in the five-component mixture (853/1144 amino acids).

5. Conclusion

The use of MALDI-IM-MS for the analysis of protein digest mixtures may significantly impact the field of proteomics. In future experiments, a more complete digestion of the sample using thermal denaturation or non-aqueous solvent systems [9–11] in combination with the internal mass calibration and decreased ion suppression effects made possible by ion mobility separation could greatly improve current methods of protein identification. The MALDI-IM-MS methodology presented herein reduces analysis times, and benefits those applications that require high throughput.

In future work, we plan to test the limits of the instrument by examining increasingly complex protein digest material. This work could impact the analysis of whole cell lysates, which can introduce non-protein impurities to the sample; however, such impurities should have very different mass–mobility relationships (trend-lines) when compared with peptides, allowing for the rapid screening of the samples. It is also feasible to develop a screening process involving selective chemical modification of a single amino acid in order to change its collision cross-section, allowing for rapid identification of proteins or peptides that contain specific amino acids. Future instrument development will focus on combining high resolution IM with high resolution TOF without sacrificing the sensitivity or limit of detection of the current technique. Clearly, ion mobility separation is a powerful tool that can be applied to a range of problems in bioanalytical chemistry.

Acknowledgements

The authors thank Dr. William K. Russell and Dr. Zee-Yong Park for their suggestions. The ion mobility research at TAMU is supported by a National Science Foundation grant (CHE-9629966) and the TAMU TOF-MS development is supported by the US Department of Energy, Division of Chemical Sciences, OBES (DE-FG03-95ER14505). The MALDI-ion mobility/o-TOF MS developed at Ionwerks Inc. was funded by a NIH phase 1 SBIR grant (1R43 GM057736-01).

References

[1] J.L. Harry, M.C. Wilkins, B.R. Herbert, N.H. Packer, Electrophoresis 21 (2000) 1071.
[2] A. Pandy, M. Matthias, Nature 405 (2000) 837.
[3] S. Hadden, Nature 404 (2000) 541.
[4] L. Hood, Book of Abstracts, 219th ACS National Meeting, 2000, BTEC-009.
[5] S. Fields, Science 291 (2001) 1221.
[6] W.J. Henzel, T.M. Billeci, J.T. Stults, S.C. Wong, C. Grimley, C. Watanabe, Proc. Natl. Acad. Sci. U.S.A. 90 (1993) 5011.
[7] O.N. Jensen, M. Wilm, A. Shevchenko, M. Mann, in: A. Link (Ed.), Methods in Molecular Biology, Humana Press, NJ, 1999.
[8] M. Wilm, A. Shevchenko, T. Houthaeve, S. Breit, L. Schweigerer, T. Fotsis, M. Mann, Nature 379 (1996) 466.
[9] Z. Park, D.H. Russell, Anal. Chem. 72 (2000) 2667.
[10] Z. Park, D.H. Russell, Anal. Chem. 73 (2001) 2558.
[11] W.K. Russell, Z. Park, D.H. Russell, Anal. Chem. 73 (2001) 2682.
[12] J.F. Holland, C.G. Enke, J. Allison, J.T. Stults, J.D. Pinkston, B. Newcome, J.T. Watson, Anal. Chem. 55 (1983) 997A.
[13] J. Ding, P.J. Vouros, Chrom. A 887 (2000) 103.
[14] A.I. Gusev, Fresenius J. Anal. Chem. 366 (2000) 691.
[15] F. Foret, H.H. Zhou, E. Gangl, B.L. Karger, Electrophoresis 21 (2000) 1363.
[16] M.E. McComb, H. Perreault, Electrophoresis 21 (2000) 1354.

[17] S.H. Kang, X. Gong, E.S. Yeung, Anal. Chem. 72 (2000) 3014.
[18] K.J. Gillig, B. Ruotolo, E.G. Stone, D.H. Russell, K. Fuherer, M. Gonin, A. Shultz, J. Anal. Chem. 72 (2000) 3965.
[19] D.H. Russell, K.J. Gillig, E.G. Stone, Z. Park, K. Fuherer, M. Gonin, A.J. Shultz, in: Proceedings of the SPIE-International Society Optical Engineering, 2000, pp. 69.
[20] E.G. Stone, B. Ruotolo, K.J. Gillig, D.H. Russell, K. Fuherer, M. Gonin, A.J. Shultz, Anal. Chem. 73 (2001) 2233.
[21] J.A. Taraszka, A.E. Counterman, D.E. Clemmer, Fresenius J. Anal. Chem. 369 (2001) 234.
[22] R. Guevremont, D.A. Barnett, R.W. Purves, Vandermey, J. Anal. Chem. 72 (2000) 4577.
[23] G.A. Eiceman, H.H. Hill, Gardea-Torresdey, J. Anal. Chem. 72 (2000) 137R.
[24] R.D. Edmondson, D.H. Russell, Mass Spectrometry of Biological Materials, 2nd Edition, Marcell Dekker, New York, 1998, pp. 29.
[25] C. Wu, W.F. Siems, J. Klasmeier, H.H. Hill, Anal. Chem. 72 (2000) 391.
[26] C.A. Srebalus, J. Li, W.S. Marshall, D.E. Clemmer, Anal. Chem. 71 (1999) 3918.
[27] C. Koster, J.A. Castoro, C.L.J. Wilkins, Am. Chem. Soc. 114 (1992) 7572.
[28] T. Solouki, K.J. Gillig, D.H. Russell, Rapid Commun. Mass Spectrom. 8 (1994) 26.
[29] J.M. Hettick, D.L. McCurdy, D.C. Barbacci, D.H. Russell, Anal. Chem. 73 (2001) 5378.
[30] http://prospector.ucsf.edu/.
[31] K.R. Clauser, P. Baker, A.L. Burlingame, Anal. Chem. 71 (1999) 2871.
[32] K.L. Busch, R.G. Cooks, in: F.W. (Ed.), Tandem Mass Spectrometry McLafferty, Wiley/Interscience, New York 1983, pp. 11.
[33] R.D. Edmondson, D.H. Russell, J. Mass Spectrom. 32 (1997) 263.
[34] C.S. Hoaglund, S.J. Valentine, C.R. Sporleder, J.P. Reilly, D.E. Clemmer, Anal. Chem. 70 (1998) 2236.
[35] Z. Park, W.K. Russell, D.H. Russell, J. Mass Spectrom., submitted.
[36] V.V. Laiko, M.A. Baldwin, A.L. Burlingame, Anal. Chem. 72 (2000) 652.
[37] E. Krause, H. Wenschuh, P.R. Jungblut, Anal. Chem. 71 (1999) 4160.